Latin American Journal of Solids and Structures
www.lajss.org

On the stability of internally pressurized thick-walled spherical and cylindrical shells made of functionally graded incompressible hyperelastic material

Abstract

In this paper, stability analysis of thick-walled spherical and cylindrical shells made of functionally graded incompressible hyperelastic material subjected to internal pressure is presented. Instability point happens in the inflation of above mentioned shells and in this paper effect of material inhomogeneity and shell thickness has been investigated. Extended Ogden strain energy function with variable material parameter is used to model the material behavior. To model inhomogeneity, we assume that material parameter varies by a power law function in the radial direction and inhomogeneity factor is a power in the power law function. Analytical method is used to find the internal pressure versus hoop extension ratio relations in explicit form for both of cylindrical and spherical shells and the non-monotonic behavior of the inflation curves is studied. Following this, profile of inflation pressure versus hoop stretch is presented and effect of the inhomogeneity and shell thickness in the onset of instability is studied. The obtained results show that the material inhomogeneity parameter and shell thickness have a significant influence on the stability of above mentioned shells. Thus with selecting a proper material inhomogeneity parameter and shell thickness, engineers can design a specific FGM hollow cylinder that can meet some special requirements.

Keywords

Hyperelasticity, Instability, functionally graded material, thick shells.

Yavar Anani[a]
Gholamhossein Rahimi[a]*

[a]Mechanical Engineering Department, Tarbiat Modares University, Tehran, Iran. E-mail: yavar_a366@yahoo.com, rahimi_gh@modares.ac.ir

*Corresponding author

http://dx.doi.org/10.1590/1679-78254322

Received July 27, 2017
In revised form October 13, 2017
Accepted October 16, 2017
Available online February 05, 2018

1 INTRODUCTION

Rubber like materials under external loading possibly display different reactions dependent on their material properties, forces and geometry. Finite deformation theory is used to describe large deformation responses of these materials. A hyperelastic material shows a nonlinear behavior which imply that its answer to the load is not directly proportional to the deformation. Different strain energy functions are used to model hyperelastic behavior of these materials and there are numerous efforts in the literature on the derivation and/or fitting of various forms of strain-energy functions, such as works of Mooney (1940), Blatz and Ko (1962), Yeoh (1993), Ogden (1972), Beatty (1987). Presenting precise constitutive model to describe hyperelastic behavior of rubber like material is the subject of a lot of researches in the recent years such as works by Anani and Alizadeh (2011), Bao et al. (2003), Silva and Bittencourt (2008), Pereira and Bittencourt (2010), Pascon and Coda (2013), Coelho et al. (2014), Santos et al. (2015), Tomita et al. (2008) and Barforooshi and Mohammadi (2016)

As functionally graded rubber is the subject of this study it should be noted that graded rubber like materials were created by Ikeda et al. (1998) in the laboratory for the first time, a while after these materials have attracted the attention of investigators for modeling these materials behavior under mechanical and geometrical boundary conditions. Some important and novel researches about analysis of inhomogeneous rubber like materials structures are presented in details by Bilgili (2003,2004), Batra (2006), Batra and Bahrami (2009), Anani and Rahimi (2015,2016).

This paper concern is about instability analysis of internally pressurized spherical and cylindrical thick shells made of isotropic functionally graded incompressible hyperelastic materials. Moreover, finding effect of material inhomogeneity and shell thickness in the onset of instability of above mentioned shells are also analyzed in this paper. Rubber-like materials experiencing large deformations, display a diversity of amazing instabilities. A review

of some of the more interesting instances has been presented in a recent paper by Gent (2005) where background literature can be found. In the context of stability of spherical and cylindrical shells, several aspects of this problem have been studied and cited here. Inflation of spherical rubber balloons has been studied by Needleman (1977). Goriely et al. (2006) have investigated stability and bifurcation of compressed elastic cylindrical tubes. Small amplitude radial oscillations of an incompressible, isotropic elastic spherical shell has been a subject of Beatty (2011) study. Rudykh et al. (2012) have researched about snap-through actuation of thick-walled electroactive balloons. Inflation and bifurcation of thick-walled compressible elastic spherical-shells has been studied by Haughton (1987). Comparison of stability and bifurcation criteria for inflated spherical elastic shells has been done by Haughton and Kirkinis (2003).

A large number of works has been done on to analyzing instability of spherical and cylindrical shell but we found that there is a gap in the literature about stability analyzing of functionally graded incompressible hyperelastic cylindrical/spherical thick shells. Therefore, in this paper we focus on instability of these shells and effect of material parameters and structural parameters are investigated, carefully.

2 Problem formulation for cylindrical shell

In this section, instability analysis of a pressurized thick-walled hollow cylindrical shell made of isotropic FG rubber like materials which is shown in Fig.1. A, B and P_i represent inner and outer radius of the shell and internal pressure, respectively. The cylinder is considered initially stress-free and presumed to be deformed statically. (R,Θ,Z) and (r,θ,z) represent reference and current configurations of cylindrical shell. The cylinder geometry in these configurations is described as follows:

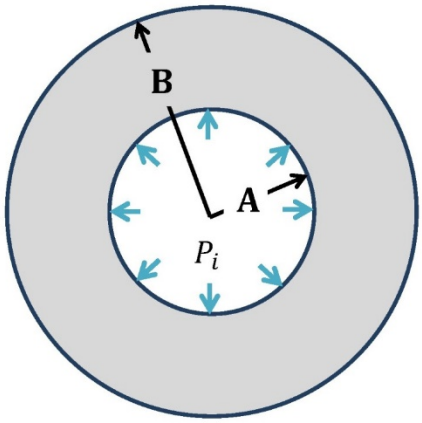

Figure 1: *Configuration of internally pressurized thick hollow cylinder*

$$A \le R \le B \ , 0 \le \Theta \le 2\pi, \ 0 \le Z \le L \tag{1}$$

$$a \le r \le \mathrm{b}, \ 0 \le \theta \le 2\pi, 0 \le z \le l \tag{2}$$

Deformation field of the cylinder can be expressed by Ericksen's proposed universal solutions (1954):

$$r = f(R), \theta = \Theta, z = \lambda_z Z \tag{3}$$

The deformation gradient tensor $\boldsymbol{F}$ is presented by (Fu and Ogden (2001)):

$$\boldsymbol{F} = \frac{\mathrm{d}f(R)}{\mathrm{d}R}\boldsymbol{e}_r \otimes \boldsymbol{E}_R + \frac{f(R)}{R}\boldsymbol{e}_\theta \otimes \boldsymbol{E}_\Theta + \lambda_z \boldsymbol{e}_z \otimes \boldsymbol{E}_Z \tag{4}$$

Radial, circumferential and axial stretches are defined by: $\lambda_r = \frac{df(R)}{dR}$, $\lambda_\theta = \frac{f(R)}{R}$, $\lambda_z = \lambda_z$ and J is determinant of the deformation gradient tensor $\boldsymbol{F}$. As the subject of this paper is incompressible hyperelastic materials, incompressibility condition indicates: $I_3 = J^2 = 1$ and it leads to:

$$\left(\lambda_r \lambda_z \lambda_\theta\right) = \left(\lambda_z f\left(\mathrm{R}\right) \mathrm{d}f\left(\mathrm{R}\right)\right) / \left(R \mathrm{d}R\right) = 1 \tag{5}$$

As a result, radial deformation of the cylinder is considered:

$$f\left(\mathrm{R}\right)^2 = \lambda_z^{-1}\left(R^2 - A^2\right) + a^2 \tag{6}$$

Cauchy stress for incompressible hyperelastic materials is stated by (Fu and Ogden (2001)):

$$\sigma_i = -p + \lambda_i \frac{\partial \hat{W}}{\partial \lambda_i} \tag{7}$$

Where p is the undetermined scalar function that explains the incompressible internal constraint conditions and $\hat{W}$ is strain energy function which is function of the principal stretches. For thick walled hollow pressurized cylinder and in the absence of body forces only one of the equilibrium equation is not satisfied identically, which is (Fu and Ogden (2001)):

$$\frac{\mathrm{d}\sigma_r}{\mathrm{d}r} + \frac{\sigma_r - \sigma_\theta}{r} = 0 \tag{8}$$

Boundary conditions are expressed by:

$$\sigma_r\left(r = a\right) = -P_i \text{ and } \sigma_r\left(r = b\right) = 0 \tag{9}$$

Substitute σ_r and σ_θ from equation (7) to equation (8) and integrating in with respect to r yields:

$$\sigma_r = -\int_a^r \left(\frac{1}{r}\left[\frac{\partial \hat{W}}{\partial \lambda_r}\lambda_r - \frac{\partial \hat{W}}{\partial \lambda_\theta}\lambda_\theta\right]\right)\mathrm{d}r - P_i \tag{10}$$

By comparison σ_r from equations (7) and (10), hydrostatic pressure is calculated as follows:

$$p = \int_a^r \left[\frac{1}{r}\left(\frac{\partial \hat{W}}{\partial \lambda_r}\lambda_r - \frac{\partial \hat{W}}{\partial \lambda_\theta}\lambda_\theta\right)\right]\mathrm{d}r + \frac{\partial \hat{W}}{\partial \lambda_r}\lambda_r + P_i \tag{11}$$

Equations (11) and (7) allow to calculate hoop stress, σ_θ, and axial stress, σ_z, by equations (12) and (13) as follows:

$$\sigma_\theta = \sigma_r + \frac{\partial \hat{W}}{\partial \lambda_\theta}\lambda_\theta - \frac{\partial \hat{W}}{\partial \lambda_r}\lambda_r \tag{12}$$

$$\sigma_z = \sigma_r + \frac{\partial \hat{W}}{\partial \lambda_z}\lambda_z - \frac{\partial \hat{W}}{\partial \lambda_r}\lambda_r \tag{13}$$

b is determined by implementing second boundary condition of equation (9):

$$P_i = -\int_a^b \left(\frac{1}{r}\left[\frac{\partial \hat{W}}{\partial \lambda_r}\lambda_r - \frac{\partial \hat{W}}{\partial \lambda_\theta}\lambda_\theta\right]\right)\mathrm{d}r \tag{14}$$

Following parameters are introduced for simplicity:

$$\beta=\frac{B}{A},\ \lambda_{(\theta)b}=\frac{b}{B},\lambda_{(\theta)a}=\frac{a}{A},\beta^2\left(\lambda_z{\lambda_{(\theta)b}}^2-1\right)=\lambda_z{\lambda_{(\theta)a}}^2-1 \tag{15}$$

With the differentiation of the strain energy function $\hat{W}$ in relation to λ_θ, denoted by $\hat{W}_{\lambda\theta}$, and with the derivative of λ_θ, $d\lambda_\theta=\frac{dr}{R}\left(1-\lambda_z\lambda_\theta^2\right)$, the equation (14) can be rewritten as follows:

$$P_i=\int_{(\lambda_\theta)_b}^{(\lambda_\theta)_a}\frac{\hat{W}_{\lambda_\theta}d\lambda_\theta}{\left(\lambda_z{\lambda_\theta}^2-1\right)} \tag{16}$$

By differentiation of equation (16) with respect to $(\lambda_\theta)_a$ and using equation (15), it is found that:

$$\frac{(\lambda_\theta)_a^{-1}\left((\lambda_\theta)_a{}^2{}_z-1\right)dP}{d(\lambda_\theta)_a}=\frac{\hat{W}_{\lambda_\theta}\left((\lambda_\theta)_a,\lambda_z\right)}{(\lambda_\theta)_a}-\frac{\hat{W}_{\lambda_\theta}\left((\lambda_\theta)_b,\lambda_z\right)}{(\lambda_\theta)_b} \tag{17}$$

Pressure turning-points at constant λ_z will exist, if $\frac{\hat{W}_{\lambda_\theta}\left((\lambda_\theta)\ ,\lambda_z\right)}{(\lambda_\theta)}$ is not monotonic in λ_θ and it leads to $\lambda_\theta\hat{W}_{\lambda_\theta\lambda_\theta}-\hat{W}_{\lambda_\theta}=0$. Modified Ogden strain energy function for incompressible materials is used as follows (Fu and Ogden (2001)):

$$\hat{W}\left(\lambda_1,\lambda_2,\lambda_3\right)=\sum_{p=1}^{N}\frac{\mu_p\left(\frac{R}{A}\right)^n}{\alpha_p}\left(\lambda_1^{\alpha_p}+\lambda_2^{\alpha_p}+\lambda_3^{\alpha_p}-3\right) \tag{18}$$

Where μ_p and α_p are material parameter which varies by power law function in radial direction $\mu_p\left(R\right)=\mu_{p0}\left(\frac{R}{A}\right)^n$, N is Number of f Ogden strain energy function sentences and n is material inhomogeneity parameter. By considering $p=1$ in relation (18), the result is defined:

$$P_i=\mu_{p0}\left(A_{OGCN}\left(b,n,\lambda_z\right)-A_{OGCN}\left(a,n,\lambda_z\right)\right) \tag{19}$$

Where:

$$A_{OGCN}\left(r,n,\lambda_z\right)=\frac{\left(\lambda_z\mathrm{r}R\right)^{-\alpha}}{\alpha_1}\left(\frac{R}{A}\right)^n\left(1-\frac{\lambda_z r^2}{\lambda_z b^2-B^2}\right)^{\frac{1}{2}(-n-\alpha)}\left(\begin{array}{l}(\mathrm{R})^{2\alpha}{}_2F_1\left(-\frac{n}{2}-\frac{\alpha}{2},-\frac{\alpha}{2};1-\frac{\alpha}{2};\frac{\lambda_z r^2}{\lambda_z b^2-B^2}\right)\\+\lambda_z^{\alpha}r^{2\alpha}\left(1-\frac{\lambda_z r^2}{\lambda_z b^2-B^2}\right)^{\alpha}{}_2F_1\left(\frac{\alpha}{2},\frac{\alpha-n}{2};\frac{\alpha+2}{2};\frac{\lambda_z r^2}{\lambda_z b^2-B^2}\right)\end{array}\right) \tag{20}$$

Where ${}_2\mathrm{F}_1(a,b;c;x)$ is the Gauss-hypergeometric function (Arfken 1985).

3 Result and Discussion

Material constants "μ_{p0}" and "α" are determined by using Levenberg–Marquardt nonlinear regression method for the rubber tested by Treloar (1944). By this method $\mu_{p0}=0.69$ and $\alpha=1.3$ are achieved. Figure 2

shows $\frac{p_i}{\mu_0}$ versus $(\lambda_\theta)_a$ for different λ_z in an approximately thin shell which its $\frac{B}{A}=1.1$. By analyzing this figure, it is found that critical pressure will increase by decreasing λ_z. Moreover related critical pressure happens in a higher $(\lambda_\theta)_a$ when λ_z decreases. Figures 3 and 4 demonstrate $\frac{p_i}{\mu_0}$ versus $(\lambda_\theta)_a$ for different λ_z in shells with $\frac{B}{A}=2$ and $\frac{B}{A}=3$, respectively. These figures show that critical pressure increases by increasing $\frac{B}{A}$. For example $\frac{p_i}{\mu_0}$ for $\frac{B}{A}=3$ and $\lambda_z=0.2$ is 1.716 times of $\frac{p_i}{\mu_0}$ for $\frac{B}{A}=2$ and $\lambda_z=0.2$. $\frac{\Delta p}{\mu_0}$ is used to as dimensionless pressure. This dimensionless pressure can be used to predict behavior of the structure without knowing its material and after that it can be used very important factor in material tailoring. In addition, critical pressure happens in a higher $(\lambda_\theta)_a$ when $\frac{B}{A}$ increases in a constant λ_z. Figure 5 shows $\frac{p_i}{\mu_0}$ versus $(\lambda_\theta)_a$ for different λ_z in a very thick shell with $\frac{B}{A}=20$. In this case, shell is very stable. For instance, instability does not occur for $\lambda_z=0.2$ even in $(\lambda_\theta)_a\approx 7$.

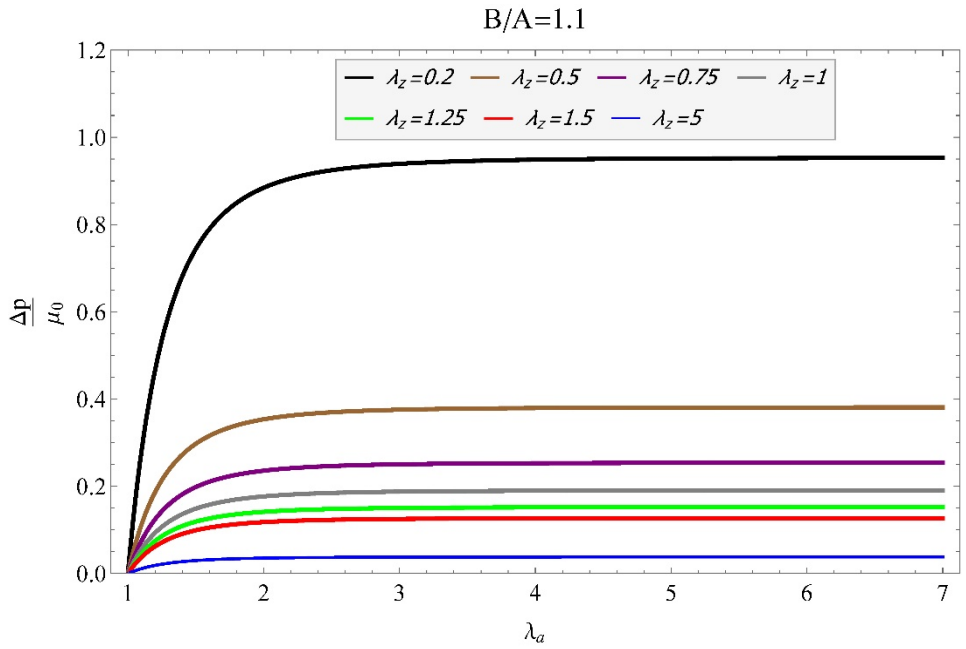

Figure 2: $\frac{p_i}{\mu_0}$ *versus* $(\lambda_\theta)_a$ *for different* λ_z*, constant material inhomogeneity parameter and* $\frac{B}{A}=1.1$

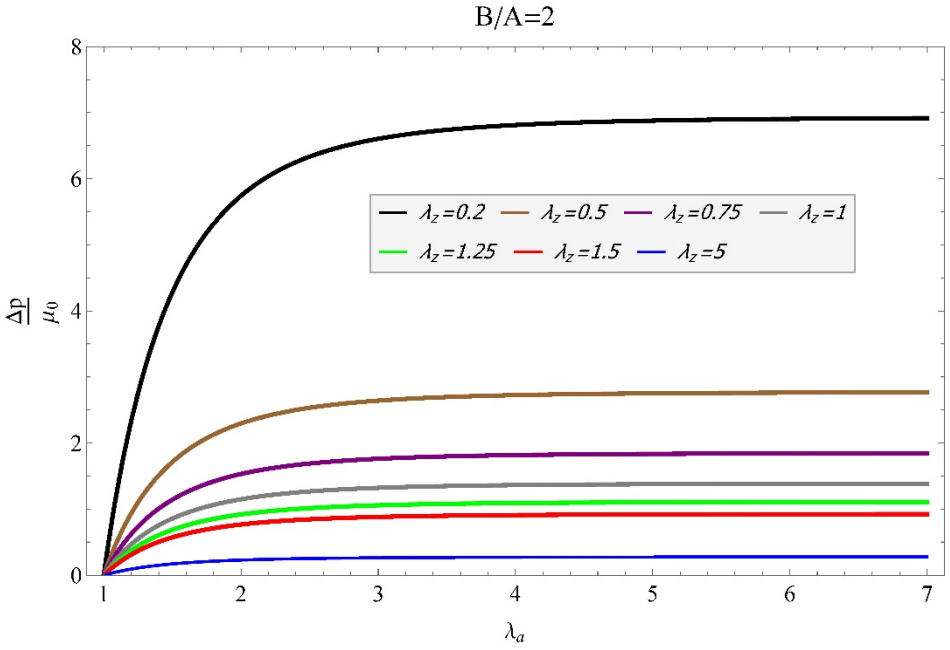

Figure 3: $\frac{p_i}{\mu_0}$ *versus* $(\lambda_\theta)_a$ *for different* λ_z *, constant material inhomogeneity parameter a nd* $\frac{B}{A}=2$

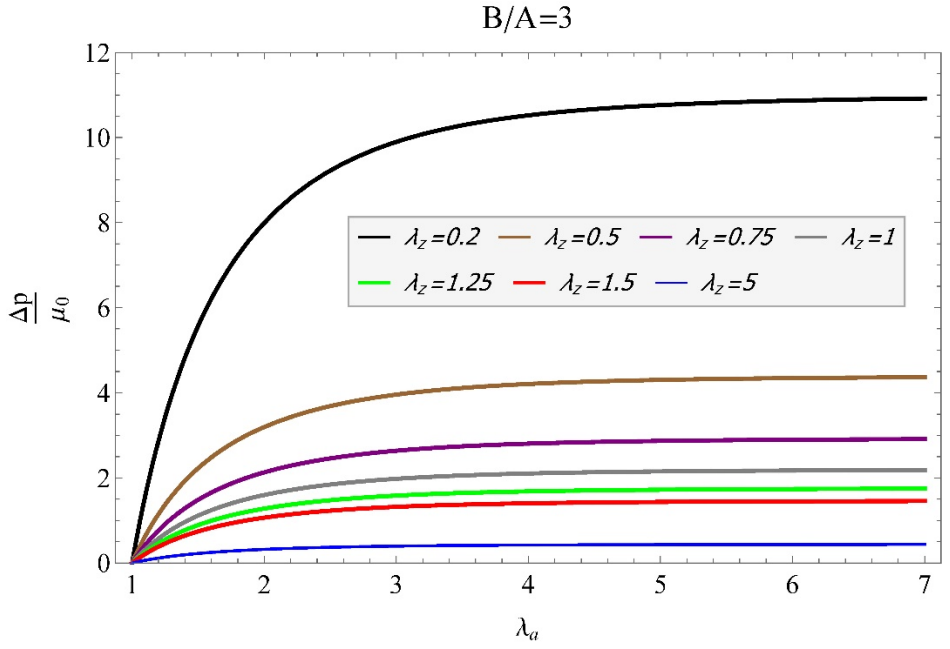

Figure 4: $\frac{p_i}{\mu_0}$ *versus* $(\lambda_\theta)_a$ *for different* λ_z *, constant material inhomogeneity parameter and* $\frac{B}{A}=3$

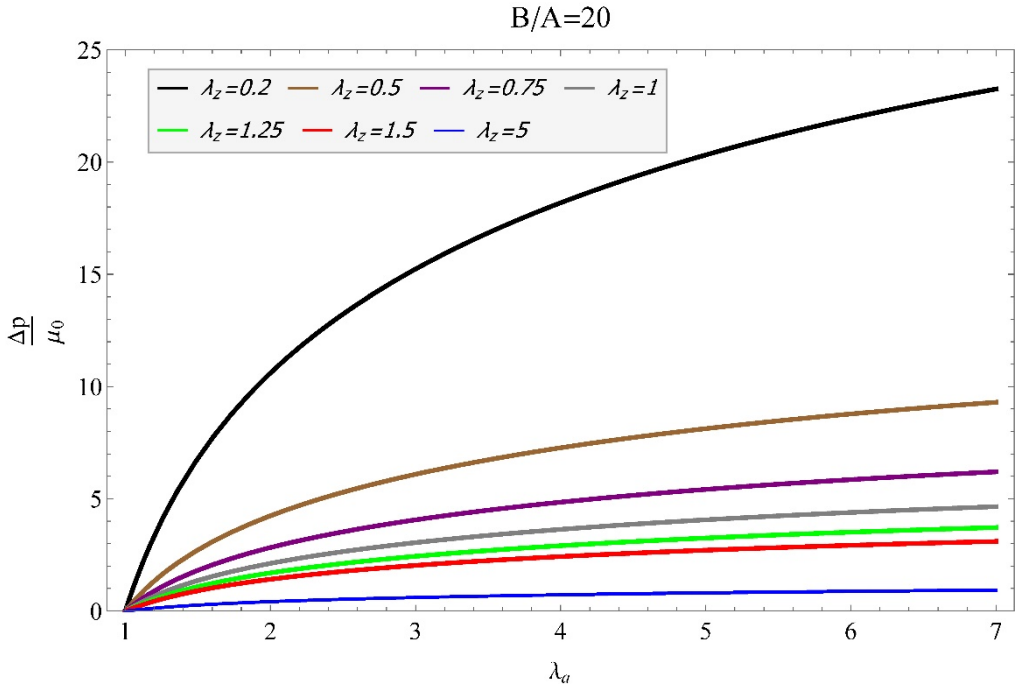

Figure 5: $\frac{p_i}{\mu_0}$ *versus* $(\lambda_\theta)_a$ *for different* λ_z *, constant material inhomogeneity parameter and* $\frac{B}{A}=20$

Figures 6, 7 and 8 show $\frac{p_i}{\mu_0}$ versus $(\lambda_\theta)_a$ by considering $\frac{B}{A}=2$ for different inhomogeneity parameter and for $\lambda_z=0.75$, 1, 1.25, respectively. These figures demonstrate critical pressure increases by increasing material inhomogeneity parameter (n). For example, ratio of critical pressure for $n=4$ and $n=0$ is 4.78. Moreover, related critical pressure happens in a higher $(\lambda_\theta)_a$ when n increases. For instance, critical pressure in figure 5 happens for $n=4$ and $n=0$ in $(\lambda_\theta)_a=5.23$ and $(\lambda_\theta)_a=2.94$, respectively.

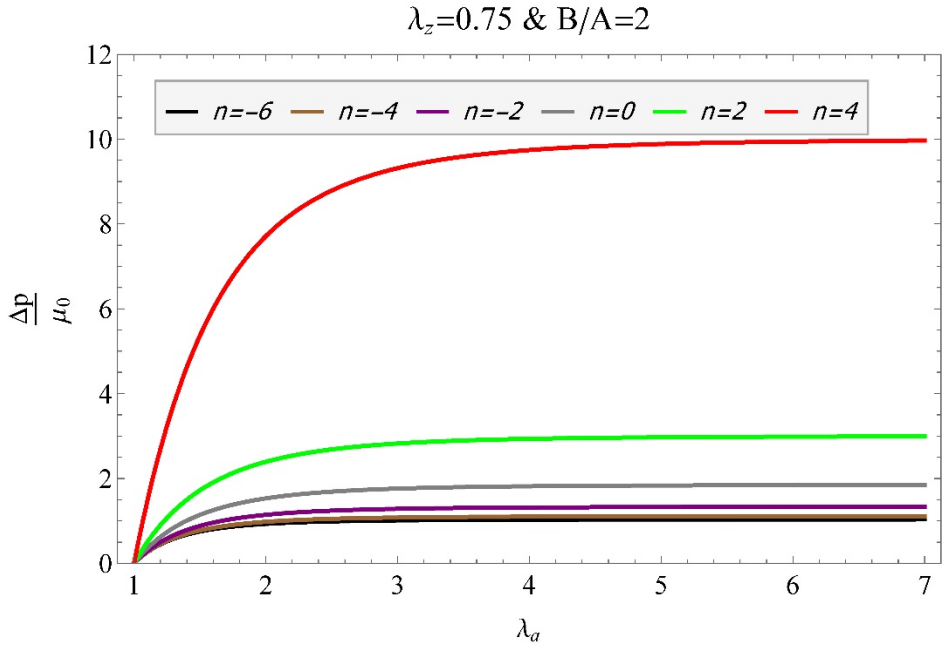

Figure 6: $\frac{p_i}{\mu_0}$ *versus* $(\lambda_\theta)_a$ *by considering* $\frac{B}{A}=2$ *for different inhomogeneity parameter and* $\lambda_z=0.75$

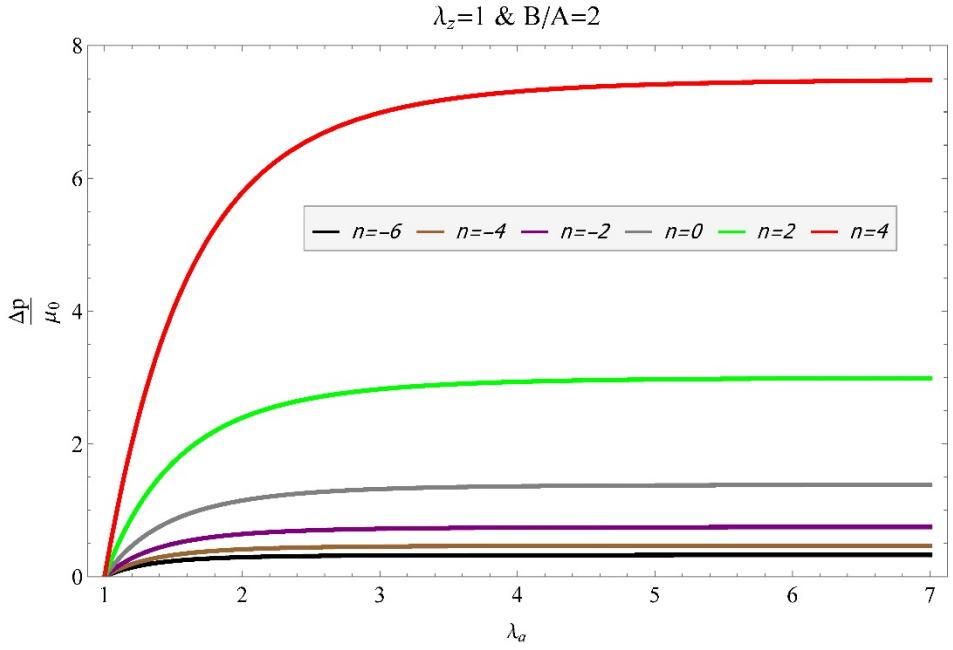

Figure 7: $\frac{p_i}{\mu_0}$ *versus* $(\lambda_\theta)_a$ *by considering* $\frac{B}{A}=2$ *for different inhomogeneity parameter and* $\lambda_z=1$

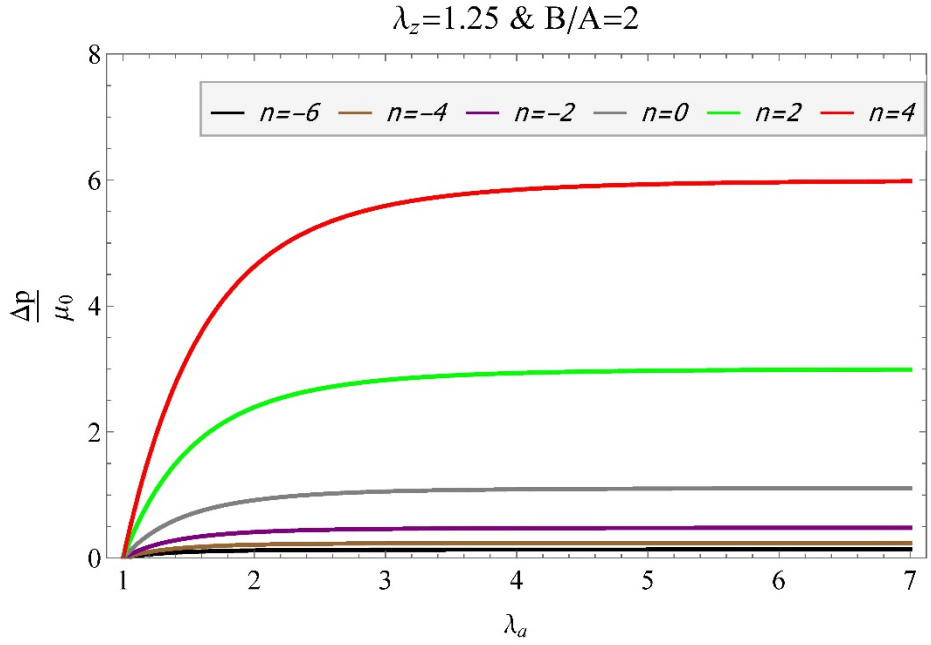

Figure 8: $\frac{p_i}{\mu_0}$ *versus* $(\lambda_\theta)_a$ *by considering* $\frac{B}{A}=2$ *for different inhomogeneity parameter and* $\lambda_z=1.25$

Figures 9, 10 and 11 show $\frac{p_i}{\mu_0}$ versus $(\lambda_\theta)_a$ for different $\frac{B}{A}$. It is very interesting to observe that for very thick shells($\frac{B}{A}=20$), instability does not occur even at $(\lambda_\theta)_a=7$. In contrast for a thin shells ($\frac{B}{A}=1.05$ *and* $\lambda_z=0.75$), instability occurs at $(\lambda_\theta)_a=1.12$.

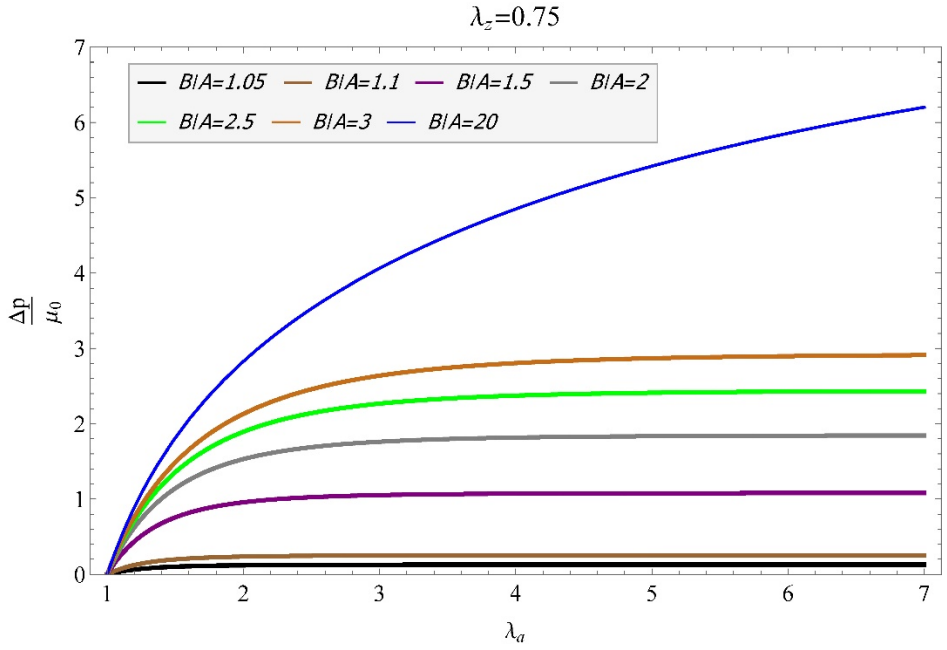

Figure 9: $\frac{p_i}{\mu_0}$ *versus* $(\lambda_\theta)_a$ *for different* $\frac{B}{A}$*, constant inhomogeneity parameter and* $\lambda_z = 1.25$

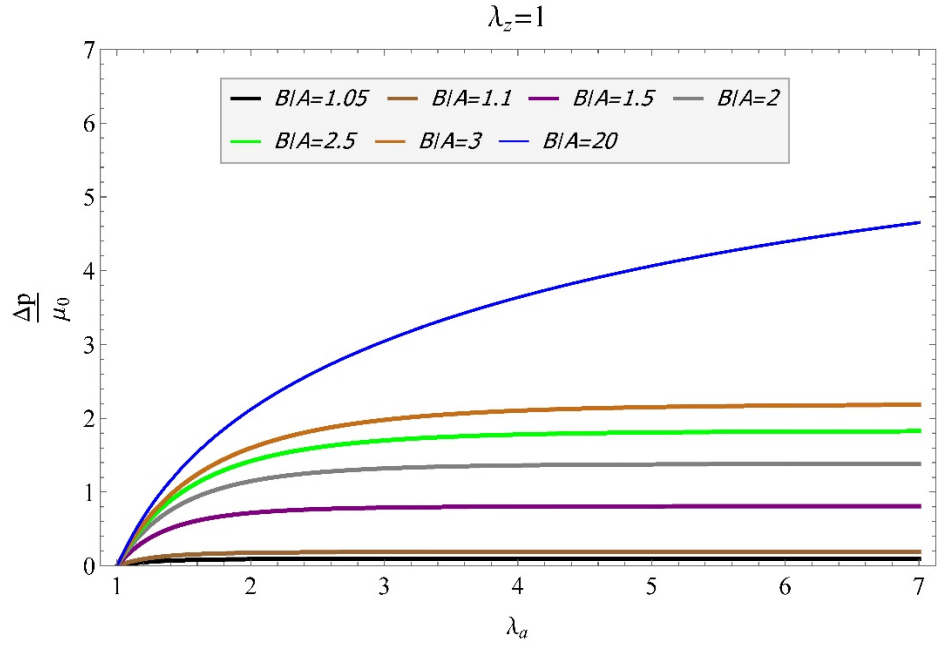

Figure 10: $\frac{p_i}{\mu_0}$ *versus* $(\lambda_\theta)_a$ *for different* $\frac{B}{A}$*, constant inhomogeneity parameter and* $\lambda_z = 1$

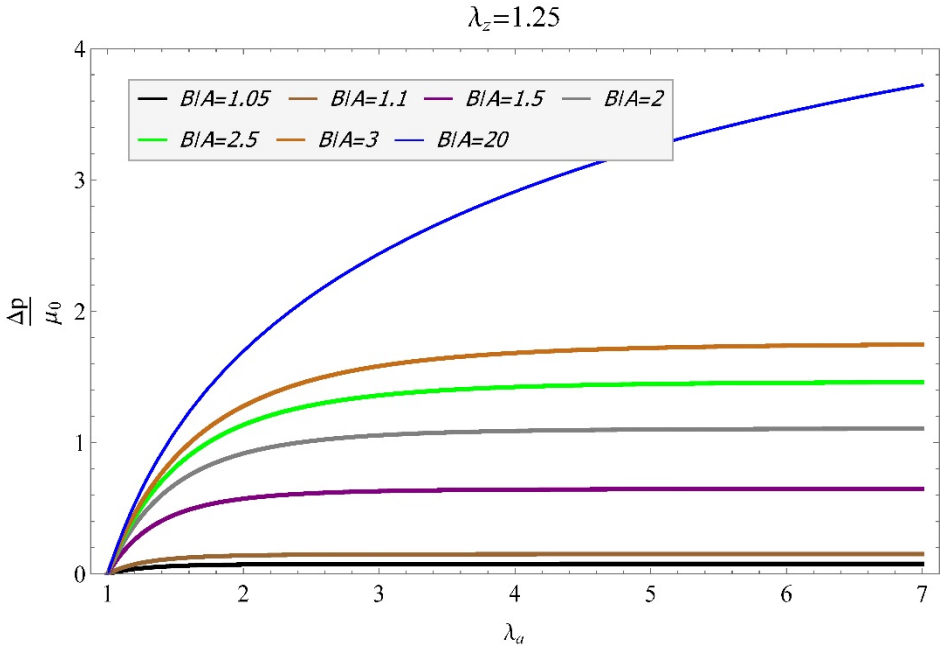

Figure 11: $\frac{p_i}{\mu_0}$ *versus* $(\lambda_\theta)_a$ *for different* $\frac{B}{A}$, *constant inhomogeneity parameter and* $\lambda_z = 1.25$

4 Problem formulation for spherical shell

In this section, instability analysis of a pressurized thick-walled hollow spherical shell made of isotropic FG rubber like materials. A, B and P_i represent inner and outer radius of the shell and internal pressure, respectively. Condition s are the same of the cylindrical shell and reference and current configurations of spherical shell are presented by (R,Θ,Φ) and (r,θ,φ). The sphere geometry in these configurations is described as follows:

$$A \le R \le B \ , 0 \le \Theta \le 2\pi, 0 \le \Phi \le 2\pi \tag{21}$$

$$\le r \le \mathrm{b},\ 0 \le \theta \le 2\pi, 0 \le \varphi \le 2\pi \tag{22}$$

Ericksen's universal solutions is used to find deformation of spherical shell (Ericksen, 1954):

$$r = f(R),\ \ \theta = \Theta, \varphi = \Phi \tag{23}$$

Components of stretch in spherical coordinates are defined as follow: $\lambda_r = \frac{df(R)}{dR}$, $\lambda_\theta = \lambda_\varphi = \frac{f(R)}{R}$ The deformation gradient tensor $\boldsymbol{F}$ is presented by (Fu and Ogden (2001)):

$$\boldsymbol{F} = \frac{\mathrm{d}f(R)}{\mathrm{d}R}\boldsymbol{e}_r \otimes \boldsymbol{E}_R + \frac{f(R)}{R}\boldsymbol{e}_\theta \otimes \boldsymbol{E}_\Theta + \frac{f(R)}{R}\boldsymbol{e}_\varphi \otimes \boldsymbol{E}_\Phi \tag{24}$$

Method which is used for the cylinder is also applied for the sphere. As a result, internal pressure is found as follows:

$$P_i = \int_{(\lambda_\theta)_b}^{(\lambda_\theta)_a} \frac{\hat{W}_{\lambda_\theta} d_{\lambda_\theta}}{\left(\lambda_\theta^{\,3} - 1\right)} \tag{25}$$

In this section, following parameters are also defined:

$$(\lambda_\theta)_a = \frac{a}{A}, (\lambda_\theta)_b = \frac{b}{B} = \left((\lambda_\theta)_a^{\,3} + \beta^3\right)^{\frac{1}{3}}, \beta, = B/A > 1,\ \beta^3\left((\lambda_\theta)_b^{\,3} - 1\right) = (\lambda_\theta)_a^{\,3} - 1 \tag{26}$$

By differentiation of equation (25) with respect to $(\lambda_\theta)_a$ and some simplification, it is found that:

$$\frac{\left((\lambda_\theta)_a-(\lambda_\theta)_a{}^{-2}\right)dP}{d(\lambda_\theta)_a}=\frac{\hat{W}_{\lambda_\theta}\left((\lambda_\theta)_a\right)}{(\lambda_\theta)_a{}^2}-\frac{\hat{W}_{\lambda_\theta}\left((\lambda_\theta)_b\right)}{(\lambda_\theta)_b{}^2} \tag{27}$$

Pressure turning-points will exist, if $\frac{\hat{W}_{\lambda_\theta}}{(\lambda_\theta)^2}$ is not monotonic in λ_θ and it leads to $\lambda_\theta\hat{W}_{\lambda_\theta\lambda_\theta}-2\hat{W}_{\lambda_\theta}=0$. By using modified Ogden strain energy function for incompressible hyperelastic material and Eq. (25), we have:

$$P_i=\mu_1\left[\left[A_{OGSN}\left(b,m\right)-A_{OGSN}\left(a,m\right)\right]\right] \tag{28}$$

Where:

$$A_{OGSN}\left(r,m\right)=\frac{3r^{-2\alpha_1}\left(R\right)^{m-\alpha_1}}{A^m\alpha_1}\left(1-\frac{r^3}{b^3-B^3}\right)^{\frac{1}{3}\left(-2\alpha_1-m\right)}$$
$$\left[R^{3\alpha_1}{}_2F_1\left(-\frac{m}{3}-\frac{2\alpha_1}{3},-\frac{1}{3}\left(2\alpha_1\right);1-\frac{2\alpha_1}{3};\frac{r^3}{b^3-B^3}\right)+2r^{3\alpha_1}\left(1-\frac{r^3}{b^3-B^3}\right)^{\alpha}{}_2F_1\left(\frac{\alpha_1}{3},\frac{\alpha_1-m}{3};\frac{\alpha_1+3}{3};\frac{r^3}{b^3-B^3}\right)\right] \tag{29}$$

5 Result and Discussion

Figures 12-14 show $\frac{p_i}{\mu_0}$ versus $(\lambda_\theta)_a$ for different inhomogeneity parameter m. By analyzing these figures, it is found that critical pressure will increase by increasing m. Moreover related critical pressure happens in a higher $(\lambda_\theta)_a$ when m increases. These figures show that critical pressure also increases by increasing $\frac{B}{A}$. In addition, Figures 15-18 show $\frac{p_i}{\mu_0}$ versus $(\lambda_\theta)_a$ for different $\frac{B}{A}$ and specific material inhomogeneity parameter in each figure. These figures show that critical pressure increases by increasing $\frac{B}{A}$. For example $\frac{p_i}{\mu_0}$ for $\frac{B}{A}=4$ and $m=-3$ is 3.52 times of $\frac{p_i}{\mu_0}$ for $\frac{B}{A}=1.1$ and $m=-3$. In addition, critical pressure happens in a higher $(\lambda_\theta)_a$ when $\frac{B}{A}$ increases.

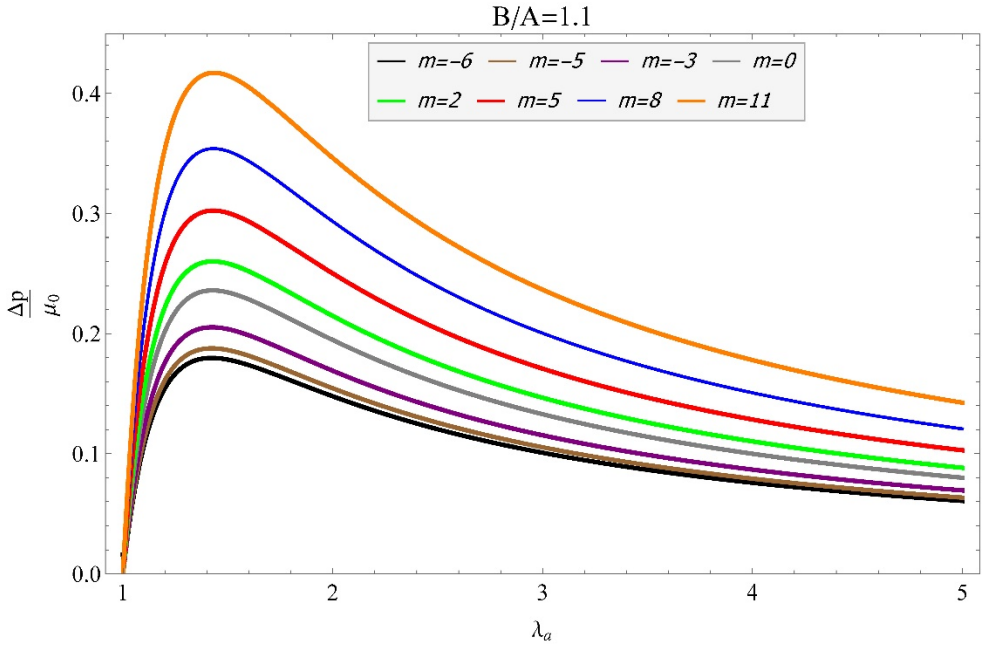

Figure 12: $\frac{p_i}{\mu_0}$ *versus* $(\lambda_\theta)_a$ *by considering* $\frac{B}{A}=1.1$ *for different inhomogeneity parameter*

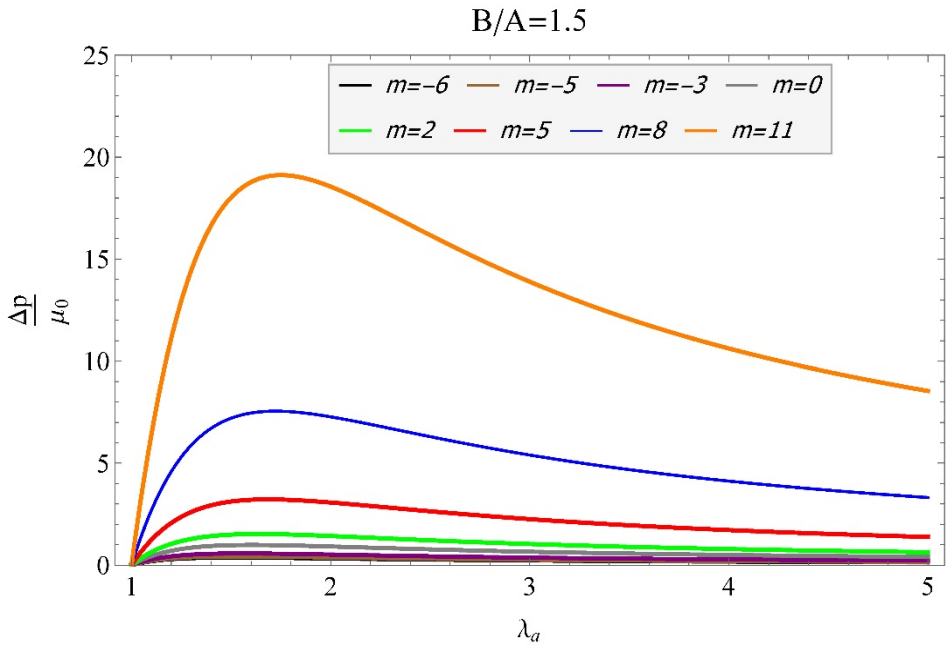

Figure 13: $\frac{p_i}{\mu_0}$ *versus* $(\lambda_\theta)_a$ *by considering* $\frac{B}{A}=1.5$ *for different inhomogeneity parameter*

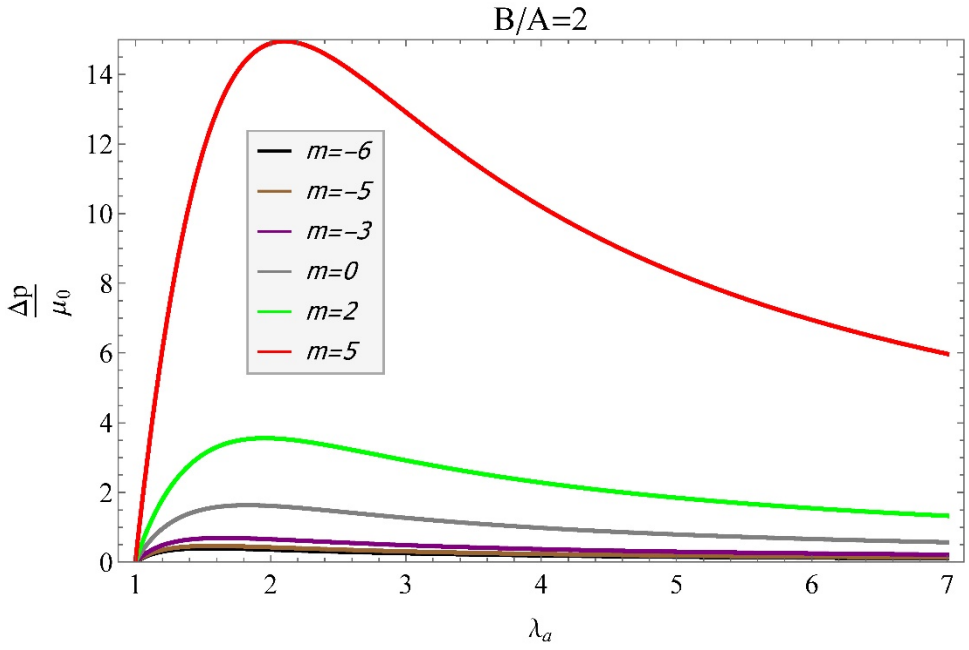

Figure 14: $\frac{p_i}{\mu_0}$ *versus* $(\lambda_\theta)_a$ *by considering* $\frac{B}{A}=2$ *for different inhomogeneity parameter*

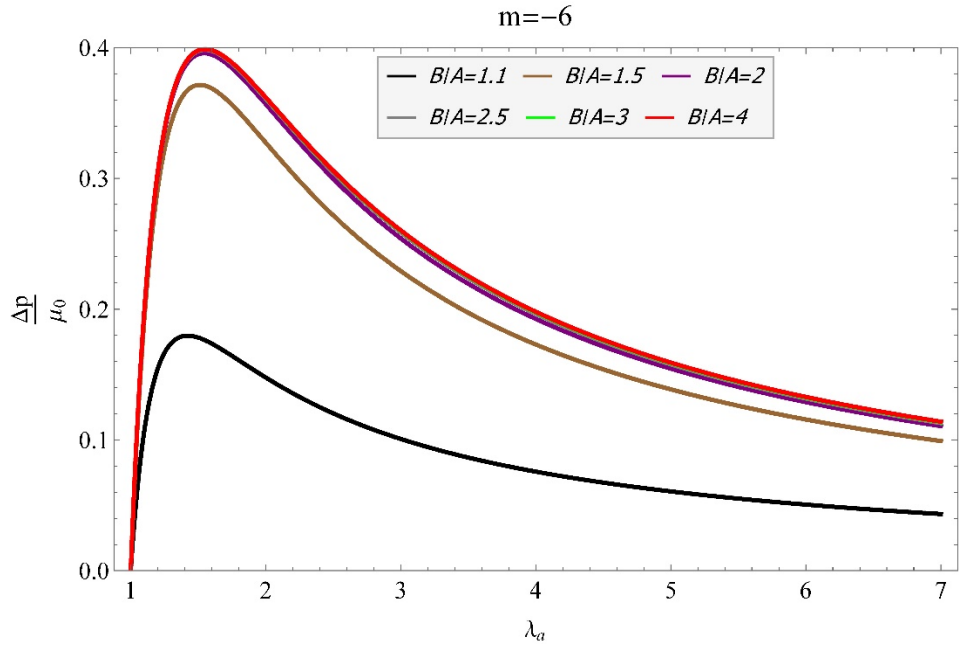

Figure 15: $\frac{p_i}{\mu_0}$ *versus* $(\lambda_\theta)_a$ *by considering* $m=-6$ *for different* $\frac{B}{A}$

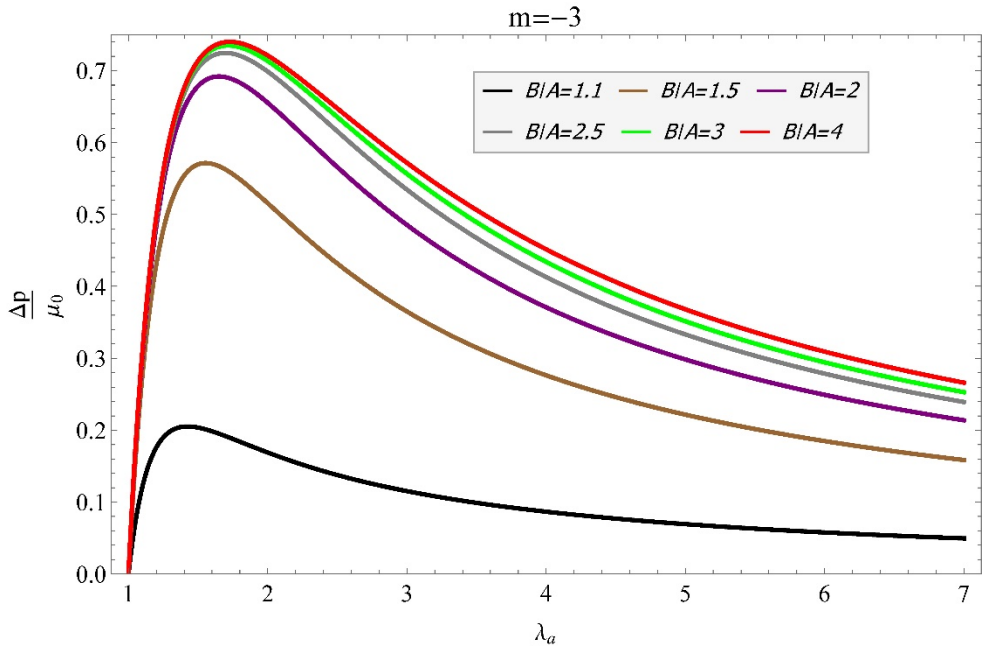

Figure 16: $\frac{p_i}{\mu_0}$ *versus* $(\lambda_\theta)_a$ *by considering* $m=-3$ *for different* $\frac{B}{A}$

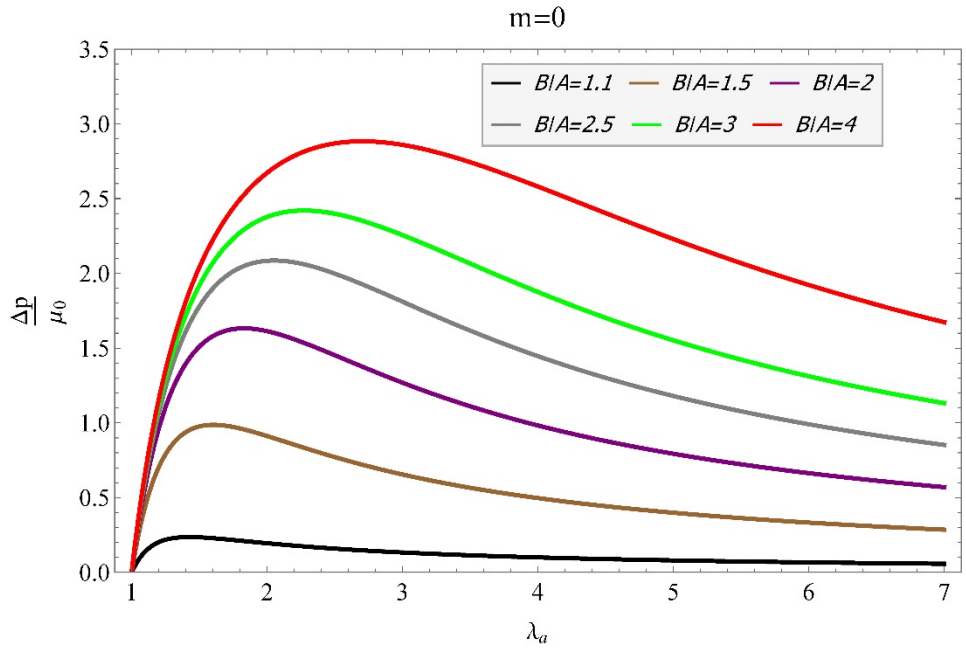

Figure 17: $\frac{p_i}{\mu_0}$ *versus* $(\lambda_\theta)_a$ *by considering* m *=0 for different* $\frac{B}{A}$

6 Validation

For validating of obtained theoretical results, numerical method is used to find the accuracy of these result. In this order sphere with $\frac{B}{A}=2$ and $m=2$ is considered. Comparison of numerical results and theoretical results is presented in Figure 19. Comparison of numerical and theoretical results shows that, maximum differences between these results are about 6.3%; therefore it is concluded that there is good agreement between numerical and theoretical results, so theoretical solution can be applied for finding stability of the axisymmetric thick vessel composed of FG hyperelastic material.

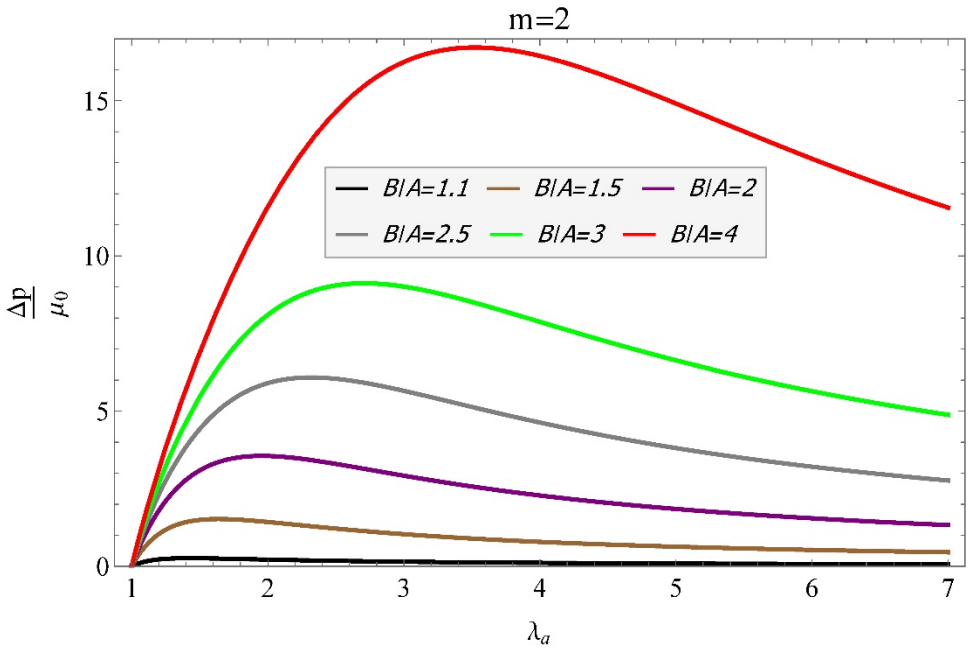

Figure 18: $\frac{p_i}{\mu_0}$ *versus* $(\lambda_\theta)_a$ *by considering* m *=2 for different* $\frac{B}{A}$

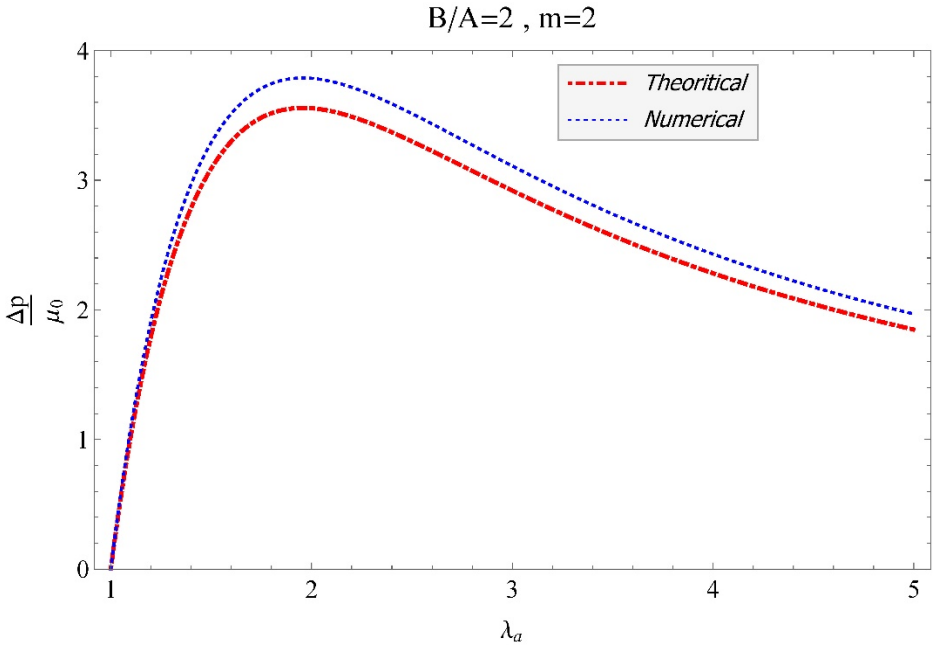

Figure 19: *Comparison between theoretical and numerical results of FG sphere*

6 Conclusion

One of the most important and amazing problems in inflated hyperelastic bodies from a hypothetical viewpoint is instability analysis and finding instability point onset of these bodies, because they happen unexpectedly. Universal solution of Ericksen's family is used to find expansion of thick spherical/cylindrical shells made of inhomogeneous, isotropic incompressible hyperelastic material. Material inhomogeneity is assumed to model by functionally graded material. Modified Ogden strain energy function with power law variable material property is used to model grading of material properties. It should be noted, Ogden material shows non-monotonic pressure-radius relationship and behaviour for cylindrical and spherical shells. Therefore, onset of instability with the predictions of effect of material inhomogeneity parameter and shell thickness is investigated.

Results show that in the thick spherical/cylindrical shell, critical internal pressure and its related hoop stretch $(\lambda_\theta)_a$ increases by increasing material inhomogeneity parameter and shell thickness. This means that, shell can tolerate higher pressure and more radial deformation. Moreover, in cylindrical shells, critical pressure and its related hoop stretch increases by decreasing longitudinal stretch. This imply that in cylindrical shell when $\lambda_z \leq 1$, longitudinal stretch has an opposite effect of internal pressure in shell behavior and instability point will be delayed by decreasing λ_z.

From an applied perspective, unstable conditions are absolutely unwelcome and should be evaded because the deformation becomes highly non-uniform, leading to early failure. Above results in investigating mechanical behavior of these shells reveal great effect of shell thickness and material inhomogeneity to delay instability and should be noted in design of these shells.

References

Anani, Y. and Alizadeh, Y., (2011), Visco-hyperelastic constitutive law for modeling of foam's behavior, J of Material& Design 32(5):2940-2948.

Anani, Y. and Rahimi G.H., (2015), Stress analysis of thick pressure vessel composed of functionally graded incompressible hyperelastic materials, International Journal of Mechanical Sciences, 104: 1-7

Anani, Y. and Rahimi G.H., (2016), Stress analysis of thick spherical pressure vessel composed of transversely isotropic functionally graded incompressible hyperelastic materials, Latin American Journal of Solid and Structures, 13: 407-434

Arfken, G., (1985), Mathematical methods for physicists, 3rd ed., Academic Press, Orlando, FL.

Bao R.H., Xue P., Yu T.X., Tao X.M. TAO (2003) Numerical simulation of large deformation of flat-topped conical shells made of textile, Latin American Journal of Solid and Structures, 1:25–47.

Barforooshi S. and Mohammadi A., (2016), Study neo-Hookean and Yeoh hyper-elastic models in dielectric elastomer-based micro-beam resonators, Latin American Journal of Solid and Structures, 13:1823–1837.

Batra, R.C. and Bahrami, A. (2009), Inflation and eversion of functionally graded nonlinear elastic incompressible cylinders, Int. J. of Non-Linear Mechanics, 44: 311–323.

Batra, R.C., (2006), Torsion of a functionally graded cylinder. AIAA J, 44:1363–1365.

Beatty, M.F., (2011), Small amplitude radial oscillations of an incompressible, isotropic elastic spherical Shell, Math. Mech. Solids.,16: 492-512.

Beatty, M.F., (1987) Topics in finite elasticity: hyperelasticity of rubber, elastomers, and biological tissues—with examples. Applied Mechanics Review 40(12): 1699-1735.

Bilgili, E., (2003), Controlling the stress–strain inhomogeneities in axially sheared and radially heated hollow rubber tubes via functional grading, Mech. Res. Commun. 30:257–66.

Bilgili, E., (2004), Modelling mechanical behaviour of continuously graded vulcanized rubbers., Plast Rubbers Compos 33(4):163–169.

Blatz, P.J. and Ko, W.L., (1962), Application of finite elastic theory to the deformation of rubbery materials. Transactions of the Society of Rheology, VI:223-252.

Coelho, M., Roehl. D. and Bletzinger. K. (2014), Numerical and analytical solutions with finite strains for circular inflated membranes considering pressure-volume coupling, International Journal of Mechanical Sciences, 82: 122-130.

Ericksen, J.L., (1954), Deformations possible in every isotropic incompressible perfectly elastic body, Z. Angew. Math. Phys. 5:466–486.

Fu,Y.B. and Ogden, R.W., (2001), Nonlinear Elasticity. Cambridge University Press.

Gent, A.N., (2005), Elastic instabilities in rubber, International Journal of Non-Linear Mechanic, 40: 165-175.

Goriely, A., Destrade, M. and Ben Amar, M., (2006), Stability and bifurcation of compressed elastic cylindrical tubes, Q. J. Mech. Appl. Math., 59: 615-630.

Haughton, D.M. and Kirkinis. E., (2003), A comparison of stability and bifurcation criteria for inflated spherical elastic shells. Math. Mech. Solids., 8: 561–572.

Haughton, D.M., (1987), Inflation and bifurcation of thick-walled compressible elastic spherical-shells. IMA J. Appl. Math., 39: 259-272.

Ikeda, Y, Kasai, Y., Murakami, S. and Kohjiya, S., (1998), Preparation and mechanical properties of graded styrene-butadiene rubber vulcanizates, J. Jpn. Inst. Metals, 62: 1013–1017.

Mooney, M., (1940), A theory of large elastic deformation, Journal of Applied Physics, 11:582-592.

Needleman, A., (1977), Inflation of spherical rubber balloons. Int. J, Solids Struct.,13: 409-421.

Ogden, R.W., (1972), Large deformation isotropic elasticity - on the correlation of theory and experiment for incompressible rubberlike solids, Proc. R.Soc. Lond. A.

Pascon J.P. and Coda H.B., (2013), Large deformation analysis of homogeneous rubber-like materials via shell finite elements, Latin American Journal of Solid and Structures, 10:1177–1210.

Pereira C.E.L. and Bittencourt M.L., (2010), Topological sensitivity analysis for a two-parameter Mooney-Rivlin hyperelastic constitutive, Latin American Journal of Solid and Structures, 7:391–411.

Rudykh, S., Bhattacharya, K. and deBotton, G., (2012), Snap-through actuation of thickwalled electroactive balloons. Int. J. Nonlinear Mech., 47: 206-209.

Santos, T., Alves, M.K. and Rossi, R. (2015), A constitutive formulation and numerical procedure to model rate effects on porous materials at finite strains, International Journal of Mechanical Sciences, 93:166-180.

Silva C.A.C. and Bittencourt M.L., (2008), Structural shape optimization of 3D nearly-incompressible hyperelasticity problems, Latin American Journal of Solid and Structures, 5:129–156.

Tomita, Y., Azuma, K. and Naito, M., (2008), Computational evaluation of strain-rate-dependent deformation behavior of rubber and carbon-black-filled rubber under monotonic and cyclic straining, International Journal of Mechanical Sciences, 50(6):856-868.

Treloar, L.R.G., (1944), Stress-strain data for vulcanised rubber under various types of deformation. Trans. Faraday Soc., 40: 59-70.

Yeoh, O.H., (1993), Some forms of the strain energy function for rubber, Rubber Chem. Technology, 66:754-771.